International Journal of Solids and Structures 167 (2019) 184–191

Contents lists available at ScienceDirect

International Journal of Solids and Structures

journal homepage: www.elsevier.com/locate/ijsolstr

Peeling mechanics of hyperelastic beams: Bending effect

Liwen He[a], Jia Lou[a], Sritawat Kitipornchai[b], Jie Yang[c,*], Jianke Du[a]

[a] Department of Mechanics and Engineering Science, Ningbo University, Ningbo, Zhejiang 315211, China
[b] School of Civil Engineering, University of Queensland, Brisbane, QLD 4072, Australia
[c] School of Engineering, RMIT University, Bundoora, VIC 3083 Australia

ARTICLE INFO

Article history:
Received 22 January 2018
Revised 28 January 2019
Available online 12 March 2019

Keywords:
Adhesion
Hyperelastic
Soft materials
Bending effect
Peeling

ABSTRACT

In this work, a new adhesion model is proposed to analyze the peeling behavior of hyperelastic beams from a rigid flat substrate by utilizing a recently developed finite strain Euler beam model and the concept of adhesion energy. Both the large strain effect and bending effect are taken into account in the model. Hence, the model can be seen as a generalization of the extensible elastica-type adhesion model to the finite strain case, and it can also be taken as a generalization of the hyperelastic membrane-type adhesion model to the hyperelastic beam case. In the modeling process, the variational method is used to derive the equilibrium equation and associated boundary conditions, including one that physically means the local peeling (fracture) criterion. A first integral is found for hyperelastic beams and it is used to derive an equivalent global peeling criterion. Moreover, an analytical formula for the peeling force during steady peeling is also obtained. Furthermore, numerical solution procedures and results are presented to discuss the effects of large strain and bending deformation on the peeling behavior of the hyperelastic beam. The developed model will contribute to the modeling and understanding of the adhesion and fracture behaviors of soft structures and biomimetic adhesives.

1. Introduction

Detachment of thin, flexible films by peeling is a ubiquitous phenomenon of practical importance to a wide range of problems. Examples include the fabrication and reliability of multifunctional layered components (Choi et al., 2005; Dupont et al., 2012), adhesive tapes used to fix objects in place (Gent and Kaang, 1986; Sun et al., 2013; Williams and Kauzlarich, 2006), transfer printing of micro/nano-scale materials and devices from one substrate to another (Feng et al., 2007; Song et al., 2009; Zaumseil et al., 2003), the ability of plants and animals to cling to surfaces (Cheng et al., 2012; Melzer et al., 2010; Pesika et al., 2007; Sauer, 2011), and the achievement of physiological functions of tissues involving cell contact, adhesion and mechanotransduction (Gao et al., 2011; Qian et al., 2017; Shao et al., 2012).

Peeling mechanics of thin films has been extensively studied (Begley et al., 2013; Chen et al., 2008; Cheng et al., 2012; Eremeyev and Naumenko, 2015; Feng et al., 2013; Gialamas et al., 2014; He et al., 2012, 2013; Kendall, 1975; Oyharcabal and Frisch, 2005; Peng and Chen, 2015a, b; Peng et al., 2010; Pesika et al., 2007; Rivlin, 1997; Sauer, 2011). Many theoretical works were conducted via employing the inextensible elastica model (Feng et al., 2013; He et al., 2012; Oyharcabal and Frisch, 2005) or extensible elastica model (He et al., 2014, 2013; Peng and Chen, 2015a, b). The finite rotation of the peeled film can be described by such kind of models, while inextensibility or small strain assumption is adopted in these models. For the case of small-angle peeling with a moderate interfacial adhesion energy or large-angle peeling with a strong interfacial adhesion energy, large strain probably occurs in the peeled film, and thus the elastica-based adhesion models fail to accurately describe the peeling behavior. The detachment of hyperelastic membranes from a flat substrate has also been studied by adopting the membrane approximation (Begley et al., 2013; Eremeyev and Naumenko, 2015; Gialamas et al., 2014; Srivastava and Hui, 2013). These adhesion models adopt hyperelastic constitutive relations and account for the large strain effect. However, the bending effect (bending resistance) is neglected in such types of models, which may be of importance in some cases (He et al., 2012, 2013; Peng and Chen, 2015a; Sauer, 2011). As far as we know, the bending effect and the large strain effect have not been simultaneously considered in a single theoretical adhesion model. The present work is motivated to propose an adhesion model with both the two effects taken into account.

It is known that hyperelastic beam models account for the bending deformation, while most hyperelastic beam models do not consider the variation of the cross-section of the beam under large strain (Attard, 2003; Simo, 1985). Thus the large strain effect is not

* Corresponding author.
E-mail addresses: heliwen@nbu.edu.cn (L. He), j.yang@rmit.edu.au (J. Yang).

https://doi.org/10.1016/j.ijsolstr.2019.03.011
0020-7683/

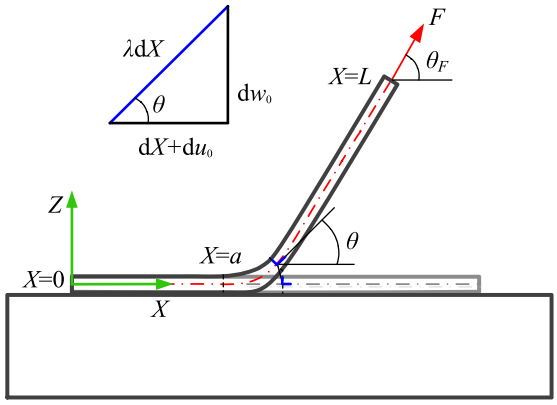

Fig. 1. Schematic figures for the reference and current configurations of a plane-strain hyperelastic beam lying on a rigid flat substrate and subjected to a peeling force.

correctly captured in these models. In a recent work (He et al., 2018), we proposed a new finite strain beam model which accounts for the thickness stretchability (with the plane strain assumption). Hence, both the bending effect and the large strain effect are captured in this model. In the present work, we will utilize this model to develop a new adhesion model so as to describe the peeling behavior of hyperelastic beams from a rigid flat substrate.

The remainder of this paper is structured as follows. In Section.2, the kinematics and constitutive relations for hyperelastic beams are firstly presented. Based on these results and by using the variational method, the equilibrium equations and associated boundary conditions are derived, including one boundary condition that physically means the local peeling criterion. A first integral is also found for the equilibrium equation, which is further utilized to derive the global peeling criterion. It is also shown in this Section that the new adhesion model can be easily degenerated to an adhesion model based on the extensible elastica theory and to another one based on the membrane approximation. In Section 3, a numerical solution procedure is proposed to analyze the un-steady peeling behavior of hyperelastic beams. Some numerical results are presented and discussed in Section 4. At last, some conclusions are draw in Section 5.

2. Theoretical modeling

2.1. Kinematics

A finite strain Euler-type beam model was proposed for hyperelastic beam structures in a previous work (He et al., 2018). We will use the model to analyze the peeling behavior of a hyperelastic beam from a rigid flat substrate. It is assumed in that model that any planar cross-section of the beam remains planar after deformation, and the deformed cross-sectional plane is still perpendicular to the deformed geometrical mid-plane. However, the rigid cross-section hypothesis usually adopted in the classical Euler beam model is relaxed by accounting for the thickness stretchability of the beam. Moreover, for simplicity, plane strain assumption is also adopted in the model. In the rest of this subsection, we will directly give the main results on the kinematics of the beam. Please refer to our previous work (He et al., 2018) for the detailed kinematic description.

An initially straight hyperelastic beam with rectangular cross-section (the width and thickness denoted by B and H, respectively) is considered. As shown in Fig. 1, the deformation of the beam from an initial (stress-free) reference configuration can be described by a mapping $\mathbf{x}=\boldsymbol{\chi}(\mathbf{X})$, or $x=X+u(X, Z)$, $y=Y$, $z=Z+w(X, Z)$ in a Cartesian coordinate system, where u and w are the horizontal and vertical displacement components of any material point in the beam, respectively. By the aforementioned deformation hypothesis, we have the following expressions for the two displacement components:

$$\begin{aligned} u(X,Z) &= u_0(X) - z^*(X,Z)sin[\theta(X)], \\ w(X,Z) &= w_0(X) + z^*(X,Z)\cos[\theta(X)] - Z, \end{aligned} \tag{1}$$

where u_0 and w_0 are the displacement components of any point on the geometrical mid plane (or simply called mid plane), $z^* = \int_0^Z \lambda_Z dZ$, in which λ_Z is the stretch of any material line element dZ and the absolute value of z^* means the deformed distance of the material point (X, Y, Z) to the mid plane, and $\theta(X)$ is the rotation angle of the deformed cross-section and is also the slanted angle of any material line element dX in the deformed mid plane. The stretch of the line element dX on the deformed mid plane is denoted by $\lambda(X)$. According to the geometric relation as shown in Fig. 1, it is easy to find that:

$$\theta = \arctan\frac{w'_0}{1+u'_0}, \lambda = \sqrt{(1+u'_0)^2 + w'^2}. \tag{2}$$

Here and thereafter, $()'$ represents derivative with respective to the reference coordinate X. In order to describe the bending deformation, the curvature of the deformed geometrical mid-plane is defined by

$$\kappa_r = \frac{d\theta}{ds} = \frac{d\theta}{\lambda dX} = \frac{\theta'}{\lambda} \tag{3}$$

where ds is the deformed length of the line element dX, and θ', denoted by κ, is the nominal curvature of the geometrical mid plane.

By adopting the incompressibility assumption, which is applicable to various kinds of materials including rubbers and biological tissues under some typical conditions (Beatty, 1987; Ogden, 1997), it was found in a previous work (He et al., 2018) that

$$\lambda_Z = \left(\lambda^2 - 2\kappa Z\right)^{-1/2}, \tag{4}$$

$$\lambda_X = \sqrt{\lambda^2 - 2\kappa Z}, \tag{5}$$

By Eqs. (4) and (5), the first principal invariant of the right Cauchy–Green deformation tensor $\mathbf{C}$ was determined:

$$I_1 = \mathrm{tr}\mathbf{C} = \lambda^2 - 2\kappa Z + \left(\lambda^2 - 2\kappa Z\right)^{-1} + 1. \tag{6}$$

Moreover, for the present homogeneous plane strain beam, the second and third principal invariants of $\mathbf{C}$ satisfy $I_2 = I_1$ and $I_3 = 1$, respectively.

2.2. Constitutive equations

For finite strain beams, the strain energy per unit reference length is defined by

$$\phi(\lambda,\kappa) = \int_A W dA, \tag{7}$$

where W is the strain energy per unit reference volume of the beam, and the area integral is over the referential (undeformed) cross-section of the beam. An energy formula for the studied thickness stretchable hyperelastic beam was also derived in the previous work (He et al., 2018), which reads:

$$\delta\phi = T\delta\lambda + M\delta\kappa. \tag{8}$$

Eq. (8) is equivalent to the following constitutive equations:

$$T = \frac{\partial\phi}{\partial\lambda}(\lambda,\kappa), M = \frac{\partial\phi}{\partial\kappa}(\lambda,\kappa), \tag{9}$$

where T and M are the stress resultant and bending moment, respectively, on the deformed cross-section. Eqs. (9) $_{1\text{-}2}$ show that

the generalized forces T and M on the cross-section are respectively work conjugated to the corresponding generalized strains λ and κ.

The Neo–Hookean model takes a very simple form,

$$W(I_1) = \frac{1}{2}\mu(I_1 - 3), \tag{10}$$

where μ is the initial shear modulus. By Eqs. (7), (9) and (10), the following constitutive equations for Neo–Hookean beams were derived:

$$\phi(\lambda,\kappa) = \frac{1}{2}\mu BH\left(\lambda^2 - 2\right) + \frac{\mu B}{4\kappa}\ln\frac{\lambda^2+\kappa H}{\lambda^2-\kappa H}, \tag{11}$$

$$\begin{aligned} T &= \mu BH\left(\lambda - \frac{1}{\lambda^3}\frac{1}{1-\kappa^2H^2/\lambda^4}\right),\\ M &= -\frac{\mu B}{4\kappa^2}\ln\frac{\lambda^2+\kappa H}{\lambda^2-\kappa H} + \frac{\mu BH}{2\kappa\lambda^2}\left(\frac{1}{1-\kappa^2H^2/\lambda^4}\right). \end{aligned} \tag{12}$$

Employing the Taylor series expansion, the following approximate constitutive equations for Neo–Hookean beams were also obtained:

$$\frac{\phi}{\mu BH} = \frac{1}{2}\left(\lambda^2 + \frac{1}{\lambda^2} - 2\right) + \frac{1}{6}\frac{\kappa^2H^2}{\lambda^6} + O\left(\xi^4\right) \tag{13}$$

$$\begin{aligned} \frac{T}{\mu BH} &= \lambda - \frac{1}{\lambda^3} - \frac{\kappa^2H^2}{\lambda^7} + O\left(\xi^4\right),\\ \frac{M}{\mu BH^3} &= \frac{1}{3}\frac{\kappa}{\lambda^6} + O\left(\xi^4\right). \end{aligned} \tag{14}$$

where ξ is defined by $\xi = \kappa H/\lambda^2$, which is usually much smaller than 1 even in the case of large rotation. These constitutive equations clearly show that in the general case of large strain, the bending and stretching deformation of Neo–Hookean beams are strongly coupled.

In the infinitesimal strain limit, both the membrane strain $\varepsilon = \lambda - 1 \ll 1$ and the bending strain $\kappa H \approx \xi \ll 1$. Thus, by truncating the Taylor series of Eq. (13) to the second order of ε and κH, it is found that $\phi = 2\mu BH\varepsilon^2 + \frac{1}{6}\mu BH^3\kappa^2$. For incompressible material under plane strain and in the infinitesimal strain limit, the Poisson's ratio $\nu = 1$ and $\mu = E/[2(1+\nu)] = E/4$. Hence, we have:

$$\phi = \frac{1}{2}EA\varepsilon^2 + \frac{1}{2}EI\kappa^2, \tag{15}$$

where $A = BH$, $EI = EBH^3/12$ and E is the Young's modulus. Eq. (15) clearly shows that in the infinitesimal strain limit, the strain energy (Eq. (13)) per unit reference length for Neo–Hookean beams recovers the classical combination of independent stretching and bending energies (without any coupling term). Similarly, it can be shown that the constitutive Eqs. (14) $_{1,2}$ for axial force and bending moment also recovers the classical $T = EA\varepsilon$ and $M = EI\kappa$ in the infinitesimal strain limit.

2.3. Governing equations and boundary conditions

The principle of stationary potential energy (Ogden, 1997) states that the total free energy E_{tot} of the beam-substrate system, consisting of the elastic energy E_{ela}, the adhesion energy E_{ad} and the external potential energy E_{ext}, reaches a minimal value when the system is at equilibrium. By the principle, we have:

$$\delta E_{tot} = \delta E_{ela} + \delta E_{ad} + \delta E_{ext} = 0. \tag{16}$$

The variation of the elastic energy of the peeled part of the beam can be written as:

$$\delta E_{ela} = \delta\int_a^L \phi \mathrm{d}X = \int_a^L (T\delta\lambda + M\delta\kappa)\mathrm{d}X - \phi(a)\delta a, \tag{17}$$

where a is the referential length of the adherent (undeformed) part of the beam and L is the total referential length of the whole hyperelastic beam.

The variation of external potential energy is:

$$\delta E_{ext} = -F_x\delta\left(a + \int_a^L \lambda\cos\theta\mathrm{d}X\right) - F_y\delta\left(\int_a^L \lambda\sin\theta\mathrm{d}X\right), \tag{18}$$

where F_x and F_y are the horizontal and vertical components of the peeling force at the end $X = L$, respectively.

The adhesion energy of the beam-substrate system is (Israelachvili, 2011):

$$\delta E_{ad} = -\omega\delta a, \tag{19}$$

where ω is the adhesion work per unit reference length at the interface between the beam and the substrate. It should be noted that any possible deformation of the adherent part of the beam is not considered here for the sake of simplicity. More complicated analysis can be conducted to discuss such an effect in the future work.

Substituting Eqs. (17)–(19) into Eq. (16), we obtain:

$$\begin{aligned} \delta E_{tot} &= \int_a^L (T\delta\lambda + M\delta\kappa)\mathrm{d}X - \phi(a)\delta a\\ &\quad - \int_a^L F_x[\delta\lambda\cos\theta - \lambda\sin\theta\delta\theta]\mathrm{d}X - \omega\delta a\\ &\quad - \int_a^L F_y[\delta\lambda\sin\theta + \lambda\cos\theta\delta\theta]\mathrm{d}X - F_x\delta a\\ &\quad + (F_x\lambda(a)\cos\theta(a) + F_y\lambda(a)\sin\theta(a))\delta a\\ &= \int_a^L \{(T - F_x\cos\theta - F_y\sin\theta)\delta\lambda\\ &\quad + \left[-M' + \lambda(F_x\sin\theta - F_y\cos\theta)\right]\delta\theta\}\mathrm{d}X\\ &\quad + M\delta\theta|_L - M\delta\theta|_a - [F_x(1-\lambda(a)\cos\theta(a))\\ &\quad - F_y\lambda(a)\sin\theta(a) + \omega + \phi(a)]\delta a \end{aligned} \tag{20}$$

Considering the arbitrariness of independent kinematic variables λ, θ and a, and using the relation $\delta\theta|_a = \delta\theta_a - \theta'(a)\delta a$ (*i.e.*, the variation of θ_a has two contributions, the one $\delta\theta|_a$ is from the variation of the function itself at an assumed fixed boundary a and the other $\theta'(a)\delta a$ is due to the variation δa of the boundary), we derive the following Euler–Lagrange equations:

$$T = F_x\cos\theta + F_y\sin\theta,\ M' + \lambda S = 0, \tag{21}$$

and associated boundary conditions:

$$\begin{aligned} M\kappa + T\lambda - F_x - \phi &= \omega, \text{ at } X = a,\\ M &= 0, \text{ at } X = L, \end{aligned} \tag{22}$$

where $S = F_y\cos\theta - F_x\sin\theta$ and it physically means the shear force on the deformed cross-section of the beam. Eqs. (21) and (22) should be supplemented with the following essential boundary condition:

$$\theta = 0, \text{at } X = a. \tag{23}$$

Actually, Eq. (21) $_2$ is the moment equilibrium equation for hyperelastic beams. It is also noted that from the fracture mechanics point of view, Eq. (22) $_2$ can be interpreted as the local peeling (or fracture) criterion, which states that the energy release rate G (the left-hand side of Eq. (22) $_1$) is equal to the adhesion work ω (or fracture energy) when the peeling front (crack front) at $X = a$ neither propagates nor recedes. Such a peeling condition does not depend on whether the peeling is activated by a force loaded or displacement loaded mode. This is completely the same as the corresponding statement in the classical textbook of fracture mechanics.

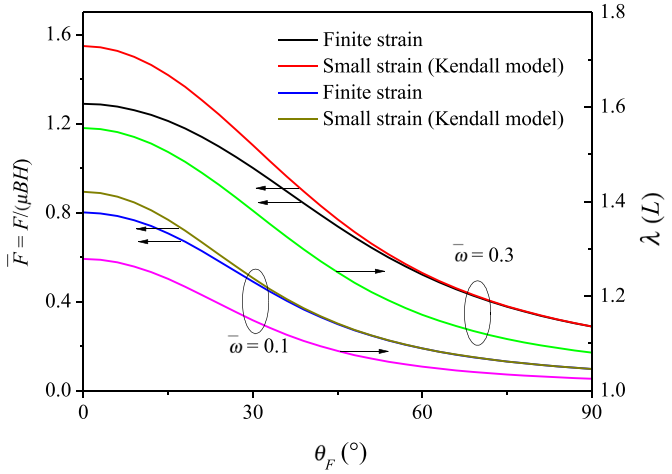

Fig. 2. Effect of the peeling angle on the peeling force and the mid-plane peeling stretch $\lambda(L)$ for the steady peeling of a plane-strain hyperelastic beam from a rigid flat substrate ($\bar{\omega} = \omega/(\mu BH)$).

With the substitution of the constitutive Eqs. (14) $_{1,2}$ into the equilibrium Eqs. (21) $_{1,2}$, we have the following equilibrium equations in terms of kinematic variables for Neo–Hookean beams:

$$\left.\begin{aligned} \mu BH\left(\lambda - \tfrac{1}{\lambda^3} - \tfrac{\theta'^2 H^2}{\lambda^7}\right) &= F\cos(\theta - \theta_F) \\ \tfrac{1}{3}\mu BH^3\left(\tfrac{\theta'}{\lambda^6}\right)' &= \lambda F \sin(\theta - \theta_F) \end{aligned}\right\} \text{for } a \le X \le L, \tag{24}$$

and corresponding boundary conditions:

$$\begin{aligned} &\theta = 0, && \text{at } X = a, \\ &\tfrac{1}{3}\mu BH^3 \tfrac{\theta'^2}{\lambda^6} + F_x(\lambda - 1) - \phi\left(\lambda, \theta'\right) = \omega, && \text{at } X = a, \\ &\theta' = 0, && \text{at } X = L, \end{aligned} \tag{25}$$

where $F = \sqrt{F_x^2 + F_y^2}$ and $\theta_F = \arctan(F_y/F_x)$ are the peeling force and peeling angle, respectively.

2.4. A first integral and a global peeling criterion

Integrating the moment equilibrium Eq. (21) $_2$ multiplied by θ' and using integration by parts, we have

$$\int_{X_1}^{X_2} \left(M' + \lambda S\right)\theta' \mathrm{d}X = (M\kappa + T\lambda)\big|_{X_1}^{X_2} - \int_{X_1}^{X_2} (M\mathrm{d}\kappa + T\mathrm{d}\lambda) = 0 \tag{26}$$

where $S = F_y\cos\theta - F_x\sin\theta$ and $T = F_x\cos\theta + F_y\sin\theta$ have been used. With the work conjugation relations $(9)_{1,2}$, Eq. (26) can be simplified to be:

$$M\kappa + T\lambda - \phi = \text{constant}. \tag{27}$$

Thus the expression $(M\kappa + T\lambda - \phi)$ is a first integral of the moment equilibrium equation for hyperelastic Euler beams, which physically means the *complementary strain energy density* (per unit reference length) of the beam. In fact, such a first integral has been extensively used to obtain solutions of integral form for inextensible elastica (He et al., 2012) or extensible elastica (He et al., 2013; Magnusson et al., 2001; Peng and Chen, 2015a) within the context of inextensibility or small strain. The present work clearly shows that *the first integral also exists for hyperelastic beams*. Moreover, the physical meaning of the first integral is more evident through such a generalization.

By using the first integral and the boundary condition $(22)_3$, the local peeling criterion $(22)_2$, which can be written as $M\kappa + T\lambda - \phi - F_X = \omega$ at $X = a$, is equivalent to the following "global" one:

$$T\lambda - \phi_m(\lambda) - F\cos\theta_F = \omega, \text{ at} X = L. \tag{28}$$

where $\phi_m(\lambda) = \phi(\lambda, 0)$. In the special case of *steady peeling*, $\theta(L) = \theta_F$, $F = T(L)$, and consequently the critical condition for steady peeling is:

$$F(\lambda - \cos\theta_F) - \phi_m(\lambda) = \omega, \text{ at } X = L, \tag{29}$$

where $\lambda(L)$ depends on the peeling force through $\mathrm{d}\phi_m/\mathrm{d}\lambda = F$.

2.5. Degenerations of the adhesion model

As given in Section 2.2, we have the following constitutive relations in the infinitesimal strain limit:

$$T = EA\varepsilon,\ M = EI\theta',\ \phi = \frac{1}{2}EA\varepsilon^2 + \frac{1}{2}EI\theta'^2$$

Hence, the governing Eq. (21) $_2$ can be degenerated to the following form:

$$EI\theta'' + \left(1 + \frac{F_x\cos\theta + F_y\sin\theta}{EA}\right)(F_y\cos\theta - F_x\sin\theta) = 0, \tag{30}$$

and associated boundary conditions (22) can also be simplified:

$$\begin{aligned} &\theta = 0, && \text{at } X = a, \\ &\tfrac{1}{2}EA\varepsilon^2 + \tfrac{1}{2}EI\theta'^2 = \omega, && \text{at } X = a, \\ &M = 0, && \text{at } X = L, \end{aligned} \tag{31}$$

which are the same with those for extensible elastica as given by He et al. (2013) and Peng and Chen (2015a). Actually, the expression for the energy release rate on the left hand side of Eq. (31) $_2$ was also stated by Suo and Hutchinson (1990), Thouless and Yang (2008) and Collino et al. (2014) among many other researchers.

When the bending effect is neglected, *i.e.*, adopting the membrane approximation, the slanted angle θ of the detached part of the beam will always be the same with the angle θ_F. By Eq. (21) $_1$ and Eq. (9) $_1$, the only governing equation in this case is:

$$\frac{\mathrm{d}\phi_m}{\mathrm{d}\lambda} = F, \tag{32}$$

where $\phi_m = \phi(\lambda, 0)$. For Neo–Hookean beams, $\phi_m = \mu BH(\lambda^2 + \lambda^{-2} - 2)/2$. Thus, the stretch λ can be uniquely determined from this equation with the assumption that ϕ_m is a monotonously increasing function of λ.

Since the bending energy vanishes and the slanted angle at the peeling front becomes θ_F (no longer vanishes) in this case, the expression for the energy release rate at the left-hand side of Eq. (22) $_2$ should be modified. Therefore, the critical condition for peeling in the membrane limit is obtained:

$$F(\lambda - \cos\theta_F) - \phi_m(\lambda) = \omega, \tag{33}$$

where the magnitude of λ depends on the peeling force F through Eq. (32). It is evident that this condition is completely the same with the one (given in Eq. (29)) for the steady peeling of hyperelastic Euler beams. It is also found that Eq. (33) recovers the condition for the peeling of hyperelastic membranes given by Eremeyev and Naumenko (2015). Actually, in the limit of inextensibility or infinitesimal strain, Eq. (33) can be easily degenerated to the classical Rivlin's formula (1997) or Kendall's formula (1973) as was done by Eremeyev and Naumenko in their work. By Eqs. (33) and (32), the critical stretch for the peeling of Neo–Hookean beams should satisfy:

$$\left(\lambda - \frac{1}{\lambda^3}\right)(\lambda - \cos\theta_F) - \frac{1}{2}\left(\lambda^2 + \frac{1}{\lambda^2} - 2\right) = \frac{\omega}{\mu BH}. \tag{34}$$

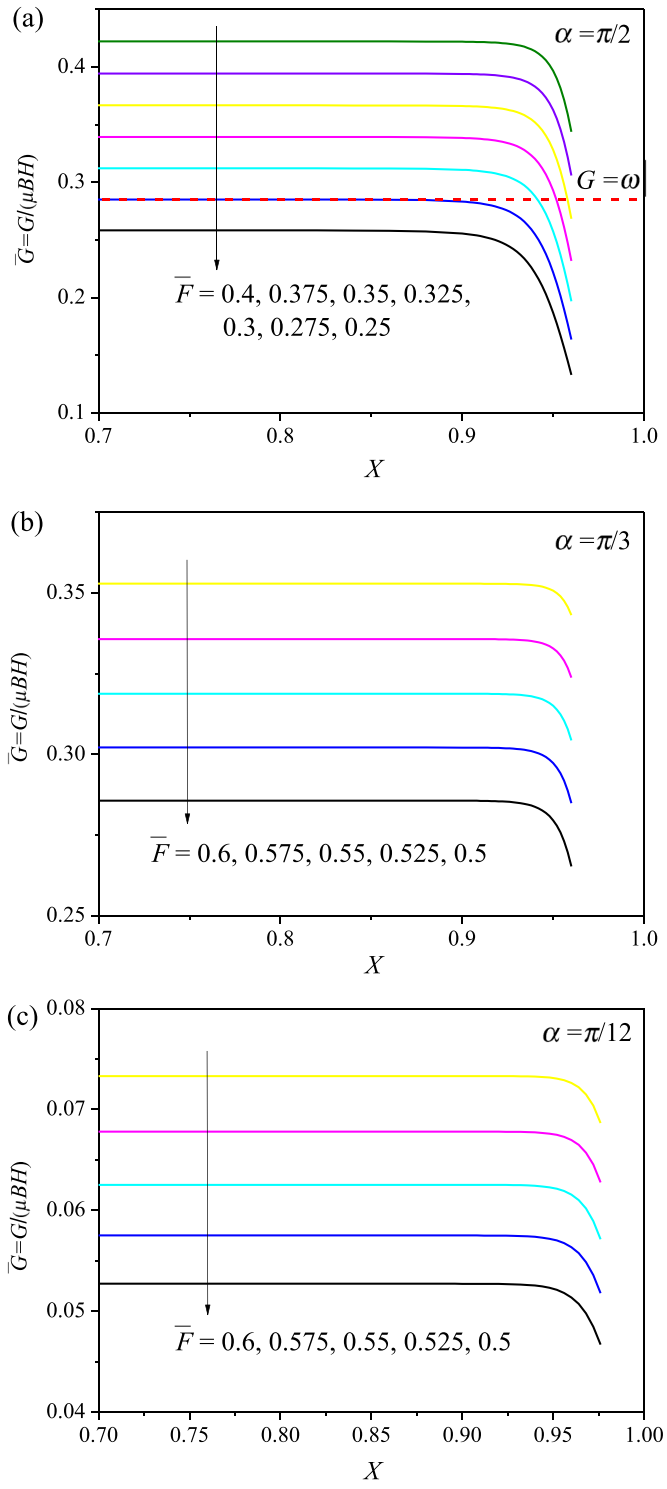

Fig. 3. Variation of the energy release rate with the position of the peeling front under specified peeling forces ($\bar{F} = F/(\mu BH)$, $H = 0.04$m, $L = 1$m): (a) $\theta_F = \pi/2$; (b) $\theta_F = \pi/3$; (c) $\theta_F = \pi/12$.

3. Numerical solution procedure

In this section, we will present a simple numerical solution procedure to the boundary value problem described in Section. 2. The solution procedure will be utilized to analyze the unsteady pealing behavior of hyperelastic beams in the next section.

With an given value for a and a specified external force F, guess an initial function $\lambda_0(X)$, utilize the finite difference method to discretize Eq. $(24)_2$ and apply the Newtonian iteration method to solve the discrete nonlinear algebraic equation together with boundary conditions $(25)_1$ and $(25)_3$, so as to obtain $\theta_1(X_j)$ ($j = 1$, 2, ..., N, with N the number of discrete points); then substitute $\theta_1(X_j)$ and its numerical derivative $(\theta_1(X_{j+1}) - \theta_1(X_j))/(X_{j+1} - X_j)$ into Eq. $(24)_1$, and solve this algebraic equation to obtain a new $\lambda_1(X_j)$; and repeat the above procedure k times until a defined error (*eg.*, $\sum_j [\theta_{k+1}(X_j) - \theta_k(X_j)]^2$ or $|\theta_{k+1}(L) - \theta_k(L)|$) is smaller than a prescribed tolerance. It is evident that such a solution procedure can be used to calculate the deformation of the membrane subjected to a specified force with a given position a of the peeling front.

However, the deformation corresponding to the given a is probably not consistent with the peeling criterion $(25)_2$. To solve such a problem, we need to evaluate the energy release rate $G = (M\theta' + F_x(\lambda - 1) - \phi)|_{X=a}$ or equivalently $G = (T\lambda - \phi_m(\lambda) - F\cos\theta_F)|_{X=L}$ (by Eq. (28)) for the given a based on the calculated deformation. If the calculated G is smaller (larger) than adhesion energy density ω, increase (decrease) the value of the external force F and then adopt the above solution procedure again; repeat the second step until the difference between G and ω is smaller than a prescribed tolerance. The final external force is the peeling force needed to peel the membrane from the given peeling front a. With the developed model and the above solution procedure, the peeling behavior of hyperelastic beams, taking Neo–Hookean beams for instance here, from a rigid flat substrate can be analyzed.

4. Results and discussion

In this section, some numerical results will be presented to discuss the effects of large strain and the bending deformation on the peeling behavior of Neo–Hookean beams.

4.1. Steady peeling

It is known that after a large enough part of a slender beam is peeled from the substrate, the slanted angle $\theta(L)$ will become equal to the peeling angle θ_F, and the peeling force will not vary in the subsequent peeling process (except the final process of complete detachment). Such a peeling process is usually called steady peeling. The peeling force for the steady peeling of adherent Neo–Hookean beams is firstly studied. The steady peeling force is calculated by using Eq. (34), and the variation of the steady peeling force with the peeling angle is plotted in Fig. 2. The results are also compared with those predicted by the classical Kendall model (1973), which is theoretically applicable in the small strain limit. It can be found that the difference between the two models is very significant when the peeling angle is small. This is due to the fact that, during the steady peeling stage, the stretch of the purely stretched part (or simply called "peeling stretch", which is just equal to the mid-plane stretch at the loading point $\lambda(L)$) of the beam increases with the decrease of the peeling angle (as displayed in Fig. 2), and consequently the large strain effect becomes more important for the small-angle peeling of hyperelastic beams. Fig. 2 also shows that the two models agree with each other in a wider range for the case of $\bar{\omega} = 0.1$ ($\bar{\omega} = \omega/(\mu BH)$), in comparison with the case of $\bar{\omega} = 0.3$. This is also because, at a given peeling angle, the peeling stretch for $\bar{\omega} = 0.1$ is smaller than that for $\bar{\omega} = 0.3$, and large strain effect is less significant for $\bar{\omega} = 0.1$. It should also be noted that the peeling force during the steady peeling stage does not rely on the bending stiffness of the beam as predicted by Eq. (29).

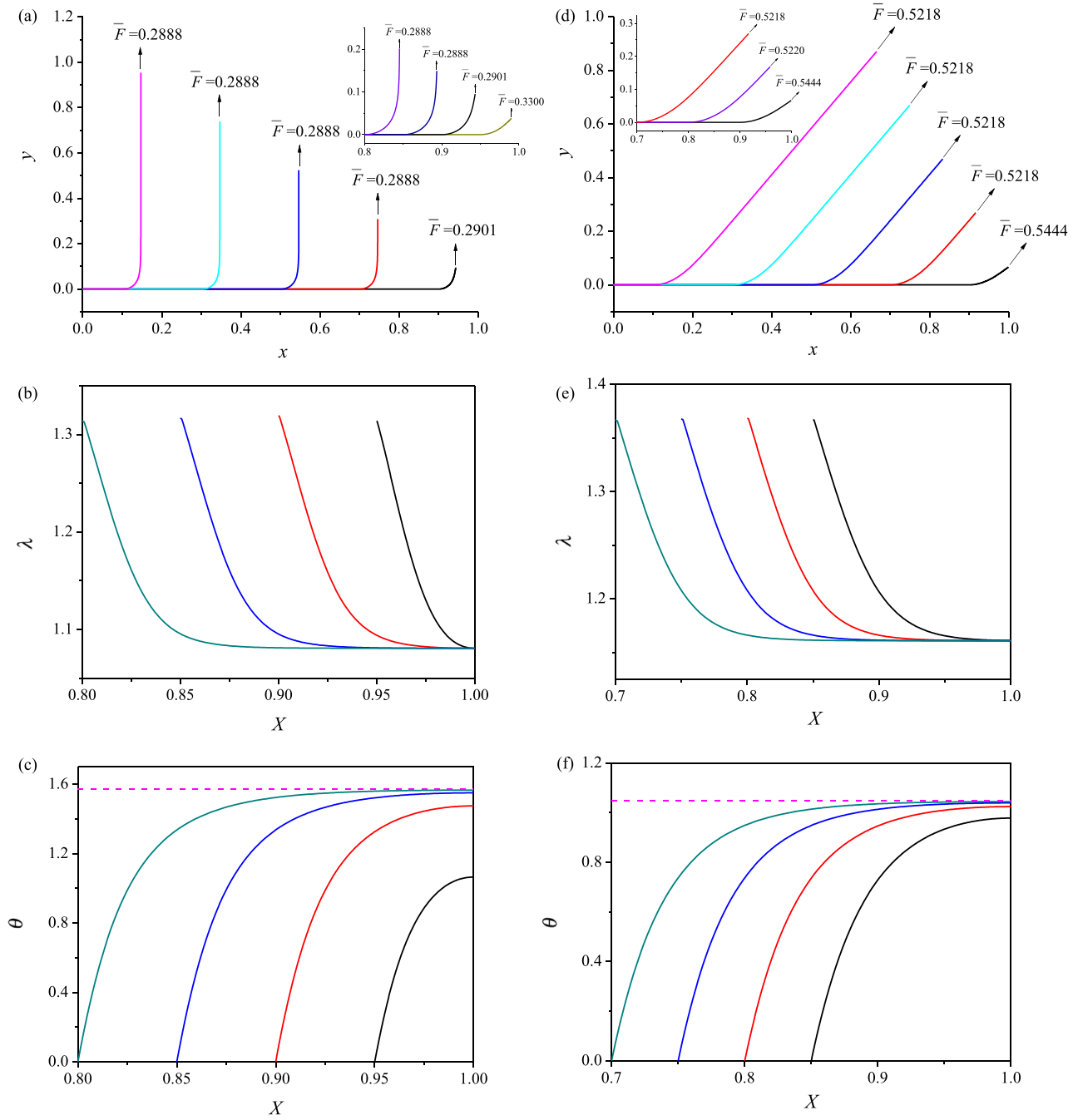

Fig. 4. The shape evolution (a, d), mid-plane stretch distribution (b, e) and local rotation distribution (c, f) of two hyperelastic beams during the peeling process from a rigid flat substrate. (a)–(c) $\bar{\omega} = 0.3$, $\theta_F = \pi/2$, $H = 0.04$m, $L = 1$m; (d)–(f) $\bar{\omega} = 0.3$, $\theta_F = \pi/3$, $H = 0.1$m, $L = 1$m. The needed peeling forces are also given in (a) and (d).

4.2. Initial peeling

The peeling process before steady peeling is termed "initial peeling" in the present work. In this subsection, the initial peeling behavior, especially the bending effect during the initial peeling, of the Neo–Hookean beam will be studied by using the adhesion model and the solution procedure presented in Sections 2 and 3.

Fig. 3 shows the variation of the energy release rate G ($\bar{G} = G/(\mu BH)$) with the position of the peeling front for a beam subjected to different peeling forces. Firstly, let's discuss the results for the case $\theta_F = \pi/2$ as shown in Fig. 3(a) for instance. Each curve in this figure displays that during steady peeling, the energy release rate does not vary with the propagation of the peeling front, while it increases significantly with the propagation of the peeling front during the initial peeling. Therefore, for an adhesion interface with a constant adhesion work ω (per unit length), the peeling criterion $G = \omega$ predicts that the needed peeling force in the initial peeling process is larger than that during steady peeling. Moreover, this figure also implicitly shows that the needed peeling force decreases with the propagation of the peeling front during the considered range of the initial peeling. The same conclusion can also be drawn for the cases $\theta_F = \pi/3$ and $\theta_F = \pi/12$, as shown in Figs. 3(b) and (c), respectively.

The shape evolution of two beams during the peeling process (including the initial peeling and steady pealing) from a rigid flat substrate are displayed in Figs. 4(a) and (d). The needed peel-

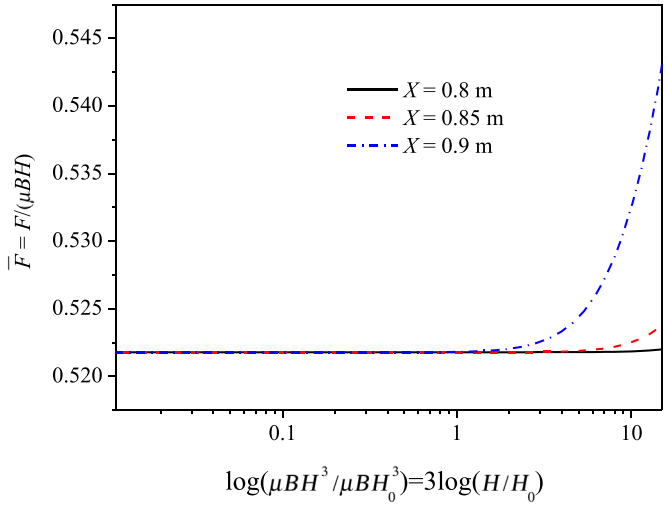

Fig. 5. Effect of the (initial) bending stiffness on the peeling force of the beam at specified positions. ($\bar{\omega} = 0.3$, $\theta_F = \pi/3$, $H_0 = 0.04$m, $L = 1$m).

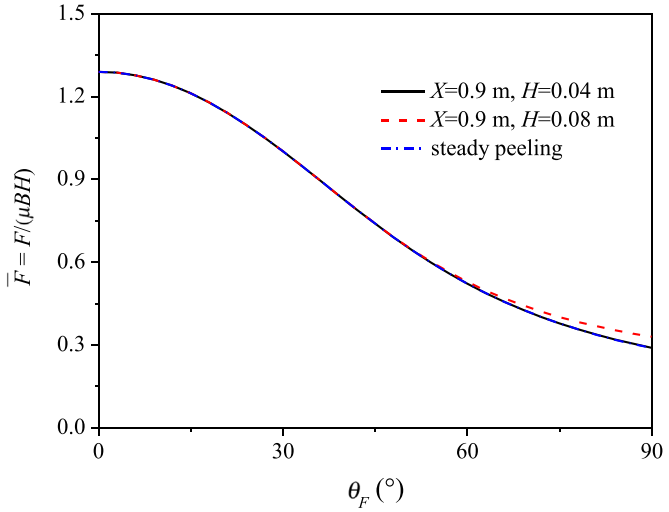

Fig. 6. Effect of the peeling angle on the peeling force at a specified position ($\bar{\omega} = 0.3$, $L = 1$m).

ing force for each configuration is also given in the two figures, from which one can directly find that the peeling force decreases with the propagation of the peeling front during the initial peeling stage. The peeled shapes of the two beams also evidently show that the bending deformation of the beam is very significant during the initial peeling stage, especially at the early stage of the initial peeling process.

Besides the peeled shapes, the distributions of the mid-plane stretch and the slanted angle for the two beams are also given in Fig. 4(b)(c) and (e)(f), respectively. The mid-plane stretch near the peeling front could be as large as 1.3 even for $\theta_F = \pi/2$ and it becomes even larger with the decrease of the peeling angle. In this case, the small-strain elastica model is not applicable, and the large strain elasticity should be employed. Moreover, in order to obtain the deformed configuration of the peeled beam during the steady or initial peeling state as shown in Fig. 4(a) and (d), the bending stiffness should also be considered. Therefore, both the large strain elasticity and bending stiffness should be accounted for to obtain the deformed configuration of a hyperelastic beam initially strongly adherent to a stiff substrate during the peeling process.

The effect of the (initial) bending stiffness on the peeling force of the Neo–Hookean beam is further discussed. Fig. 5 shows the peeling force when the peeling front propagates to three different positions ($X = 0.8$, 0.85, 0.9m). It can be found that, for a specified peeling front, when the bending stiffness is large enough, the peeling force is larger than the corresponding steady peeling force. It is demonstrated through the comparison among the three curves in this figure that, for a given bending stiffness (or given thickness), the closer the peeling front is to the peeling end ($X = 1$m) of the beam, the larger the contribution of the bending effect to the peeling force will be. Actually, besides the bending stiffness, the large strain elasticity should also be considered in order to correctly predict the peeling force at the initial peeling stage for a beam strongly adherent to a stiffness substrate with a comparatively small peeling angle. This point can be explained as follows. Firstly, it can be found from Fig. 2 that when a beam strongly adherent to a stiff substrate is peeled with a comparatively small peeling angle (should not be too small, as in that case the interface sliding probably dominates the interface failure (Collino et al., 2014)), the large strain effect significantly influences the steady peeling force. Secondly, as depicted in Fig. 3, the peeling force during the initial peeling stage monotonically approaches to the steady peeling force with the propagation of the peeling front, although the latter does not rely on the bending stiffness. Considering these two points as well as the bending effect revealed in Fig. 5, one can conclude that both the large strain effect and the bending effect should be accounted for so as to predict the peeling force for the considered case.

The effect of the peeling angle on the peeling force at a specified peeling front ($X = 0.9$m) is depicted in Fig. 6. The corresponding peeling force for steady peeling is also plotted in this figure. By considering the two cases $X = 0.9$m, H=0.04mand $X = 0.9$m, H=0.08m, we know that the former case has a thinner thickness and thus a much smaller initial bending stiffness. Via comparison among the curves for the two cases and that for steady peeling, it is easy to find that at a specified peeling front, the peeling force for the case $X = 0.9$m, H=0.04m, *i.e.*, for a beam with a comparatively small bending stiffness, is almost the same with that for steady peeling for any peeling angle; while when the peeling angle is close to $\pi/2$, the difference between the peeling force for $X = 0.9$m, H=0.08m, *i.e.*, a beam with a comparatively large bending stiffness, and that for steady peeling is considerable. This is because only in this case the bending effect is significant, and in other cases, the peeling at the peeling front $X = 0.9$m has already "entered" into the steady peeling stage. However, this does not mean that the bending effect is negligible for the case of small-angle initial peeling. As long as the peeling front is close enough to the peeling end, the bending effect should be taken into account during the initial peeling stage, even if the peeling angle is small.

At last, it should be pointed out that at the very initial peeling stage, peeling (or crack) should be initiated at the end of the completely adhered hyperelastic beam. For such a process, the present beam theory should be replaced by a finite deformation elasticity theory (Krishnan et al., 2008; Long and Hui, 2015), and the exact cohesion-separation relation on the interface should be adopted rather than the present adhesion energy concept (Oyharcabal and Frisch, 2005; Peng and Chen, 2015a; Peng et al., 2010), so as to obtain quantitatively accurate results. Moreover, when the length-to-thickness ratio of the peeled part is comparatively small, shear deformable finite strain beam models instead of the present one can be utilized to model the peeling behavior, in order to give more accurate predictions. Although the present model could not predict the peeling initiation process or give very accurate results especially for a peeled beam with small length-to-thickness ratio, both the large strain effect and the bending effect can be correctly predicted by the model, at least semi-quantitatively. The present adhesion model will be useful for evaluating the peeling and fracture behaviors of soft structures and devices.

5. Conclusion

The peeling behavior of hyperelastic beams from a rigid flat substrate is studied in the present work. By utilizing a previously developed finite strain Euler beam model and the concept of adhesion energy, a new adhesion model is established via the standard variational method to describe the peeling behavior. The novelty of the model lies in that both the large strain effect and the bending effect are taken into account in a single model. Hence, it can be taken as a generalization of the extensible elastica-type adhesion model and also an extension of the adhesion model based on the membrane approximation.

With the derived governing equations and boundary conditions, a first integral is found for the hyperelastic beam. Based on the first integral, a global peeling criterion for the adherent hyperelastic beam is derived and an analytical formula for the peeling force for steady peeling is obtained. Furthermore, a numerical solution procedure and numerical results for the general peeling process are also presented. It is found that the large strain effect is significant at small-angle peeling, and thus the Kendall model is not applicable and the derived analytical formula for steady peeling can be used instead. It is also revealed that, during the initial peeling process (before steady peeling), the bending effect has to be considered since it leads to the increase of the needed peeling force. Moreover, both the large strain elasticity and bending stiffness should be considered when predicting the small-angle peeling force during the initial peeling stage for a beam strongly adherent to a stiff substrate. The developed model and the obtained physical insights on the large strain and bending effects will contribute to the modeling, analysis and understanding of the adhesion and fracture behaviors of soft structures and devices.

Acknowledgements

The present work is supported by National Natural Science Foundation of China (Grant Nos. 11602118 and 11602117) and also sponsored by K.C. Wong Magna Fund in Ningbo University.

References

Attard, M.M., 2003. Finite strain–beam theory. Int. J. Solids Struct. 40 (17), 4563–4584.
Beatty, M.F., 1987. Topics in finite elasticity: hyperelasticity of rubber, elastomers, and biological tissues–with examples. ApMRv 40 (12), 1699–1734.
Begley, M.R., Collino, R.R., Israelachvili, J.N., McMeeking, R.M., 2013. Peeling of a tape with large deformations and frictional sliding. J. Mech. Phys. Solids 61 (5), 1265–1279.
Chen, B., Wu, P., Gao, H., 2008. Pre-tension generates strongly reversible adhesion of a spatula pad on substrate. J. R. Soc. Interface 6, 529–537.
Cheng, Q., Chen, B., Gao, H., Zhang, Y., 2012. Sliding-induced non-uniform pre-tension governs robust and reversible adhesion: a revisit of adhesion mechanisms of geckos. J. R. Soc. Interface 9 (67), 283–291.
Choi, J.-h., Kim, D., Yoo, P.J., Lee, H.H., 2005. Simple detachment patterning of organic layers and its application to organic light-emitting diodes. Adv. Mater. 17 (2), 166–171.
Collino, R.R., Philips, N.R., Rossol, M.N., McMeeking, R.M., Begley, M.R., 2014. Detachment of compliant films adhered to stiff substrates via van der Waals interactions: role of frictional sliding during peeling. J. R. Soc. Interface 11, 20140453:1-10.
Dupont, S.R., Oliver, M., Krebs, F.C., Dauskardt, R.H., 2012. Interlayer adhesion in roll-to-roll processed flexible inverted polymer solar cells. Sol. Energy Mater. Sol. Cells 97, 171–175.
Eremeyev, V.A., Naumenko, K., 2015. A relationship between effective work of adhesion and peel force for thin hyperelastic films undergoing large deformation. MeReC 69, 24–26.
Feng, X., Cheng, H., Bowen, A.M., Carlson, A.W., Nuzzo, R.G., Rogers, J.A., 2013. A finite-deformation mechanics theory for kinetically controlled transfer printing. J. Appl. Mech. 80 (6), 061023.
Feng, X., Meitl, M.A., Bowen, A.M., Huang, Y., Nuzzo, R.G., Rogers, J.A., 2007. Competing fracture in kinetically controlled transfer printing. Langmuir 23 (25), 12555–12560.
Gao, H., Qian, J., Chen, B., 2011. Probing mechanical principles of focal contacts in cell–matrix adhesion with a coupled stochastic–elastic modelling framework. J. R. Soc. Interface 8 (62), 1217–1232 rsif20110157.
Gent, A., Kaang, S., 1986. Pull-off forces for adhesive tapes. J. Appl. Polym. Sci. 32, 4689–4700.
Gialamas, P., Völker, B., Collino, R.R., Begley, M.R., McMeeking, R.M., 2014. Peeling of an elastic membrane tape adhered to a substrate by a uniform cohesive traction. Int. J. Solids Struct. 51 (18), 3003–3011.
He, L., Lou, J., Dong, Y., Kitipornchai, S., Yang, J., 2018. Variational modeling of plane-strain hyperelastic thin beams with thickness stretching effect. Acta Mech. 229 (12), 4845–4861.
He, L., Yan, S., Chu, J., 2014. Directional adhesion of gecko-inspired two-level fibrillar structures. Eur. J. Mech. – A/Solids 47, 246–253.
He, L., Yan, S., Li, B., Chu, J., 2012. Directional adhesion behavior of a single elastic fiber. J. Appl. Phys. 112 (1), 013516.
He, L., Yan, S., Li, B., Zhao, G., Chu, J., 2013. Adhesion model of side contact for an extensible elastic fiber. Int. J. Solids Struct. 50 (16–17), 2659–2666.
Israelachvili, J.N., 2011. Intermolecular and Surface Forces. Academic press.
Kendall, K., 1973. Peel adhesion of solid films-the surface and bulk effects. J. Adhes. 5 (3), 179–202.
Kendall, K., 1975. Thin-film peeling-the elastic term. J. Phys. D: Appl. Phys. 8 (13), 1449.
Krishnan, V.R., Hui, C.Y., Long, R., 2008. Finite strain crack tip fields in soft incompressible elastic solids. Langmuir 24 (24), 14245–14253.
Long, R., Hui, C.-Y., 2015. Crack tip fields in soft elastic solids subjected to large quasi-static deformation – a review. Extreme Mech. Lett. 4, 131–155.
Magnusson, A., Ristinmaa, M., Ljung, C., 2001. Behaviour of the extensible elastica solution. Int. J. Solids Struct. 38 (46–47), 8441–8457.
Melzer, B., Steinbrecher, T., Seidel, R., Kraft, O., Schwaiger, R., Speck, T., 2010. The attachment strategy of English ivy: a complex mechanism acting on several hierarchical levels. J. R. Soc. Interface 7 (50), 1383–1389.
Ogden, R.W., 1997. Non-linear Elastic Deformations. Courier Corporation.
Oyharcabal, X., Frisch, T., 2005. Peeling off an elastica from a smooth attractive substrate. Physical Review E, 71, 036611.
Peng, Z., Chen, S., 2015a. Effect of bending stiffness on the peeling behavior of an elastic thin film on a rigid substrate. Phys. Rev. E 94 (4), 042401.
Peng, Z., Chen, S., 2015b. Peeling behavior of a thin-film on a corrugated surface. Int. J. Solids Struct. 60, 60–65.
Peng, Z., Chen, S., Soh, A., 2010. Peeling behavior of a bio-inspired nano-film on a substrate. Int. J. Solids Struct. 47 (14–15), 1952–1960.
Pesika, N.S., Tian, Y., Zhao, B., Rosenberg, K., Zeng, H., McGuiggan, P., Autumn, K., Israelachvili, J.N., 2007. Peel-zone model of tape peeling based on the gecko adhesive system. J. Adhes. 83 (4), 383–401.
Qian, J., Lin, J., Xu, G.-K., Lin, Y., Gao, H., 2017. Thermally assisted peeling of an elastic strip in adhesion with a substrate via molecular bonds. J. Mech. Phys. Solids 101, 197–208.
Rivlin, R.S., 1997. The effective work of adhesion. In: Collected Papers of RS Rivlin. Springer, pp. 2611–2614.
Sauer, R.A., 2011. The peeling behavior of thin films with finite bending stiffness and the implications on gecko adhesion. J. Adhes. 87 (7–8), 624–643.
Shao, D., Levine, H., Rappel, W.-J., 2012. Coupling actin flow, adhesion, and morphology in a computational cell motility model. In: Proceedings of the National Academy of Sciences, 109, pp. 6851–6856.
Simo, J.C., 1985. In: A finite strain beam formulation. The three-dimensional dynamic problem. Part I, 49. CMAME, pp. 55–70.
Song, L., Ci, L., Gao, W., Ajayan, P.M., 2009. Transfer printing of graphene using gold film. ACS Nano 3 (6), 1353–1356.
Srivastava, A., Hui, C.-Y., 2013. Large deformation contact mechanics of a pressurized long rectangular membrane. II. Adhesive contact. Proc. R. Soc. A. 469 (2160), 20130425.
Sun, S., Li, M., Liu, A., 2013. A review on mechanical properties of pressure sensitive adhesives. Int. J. Adhes. Adhes. 41, 98–106.
Suo, Z., Hutchinson, J.W., 1990. Interface crack between two elastic layers. Int. J. Fract. 43 (1), 1–18.
Thouless, M., Yang, Q., 2008. A parametric study of the peel test. Int. J. Adhes. Adhes. 28 (4–5), 176–184.
Williams, J.A., Kauzlarich, J.J., 2006. The influence of peel angle on the mechanics of peeling flexible adherends with arbitrary load–extension characteristics. Tribol. Int. 38 (11–12), 951–958.
Zaumseil, J., Meitl, M.A., Hsu, J.W., Acharya, B.R., Baldwin, K.W., Loo, Y.-L., Rogers, J.A., 2003. Three-dimensional and multilayer nanostructures formed by nanotransfer printing. Nano Lett. 3 (9), 1223–1227.